

Spectroscopic evidence of a topological quantum phase transition in ultrathin Bi₂Se₃ films

Yusuke Sakamoto,¹ Toru Hirahara,^{1,*} Hidetoshi Miyazaki,² Shin-ichi Kimura,² and Shuji Hasegawa¹
¹*Department of Physics, University of Tokyo, 7-3-1 Hongo, Bunkyo-ku, Tokyo 113-0033, Japan*
²*UVSOR Facility, Institute for Molecular Science, Okazaki 444-8585, Japan*

(Received 23 February 2010; revised manuscript received 30 March 2010; published 22 April 2010)

We have measured the band dispersion of ultrathin Bi₂Se₃ films formed on a silicon substrate using angle-resolved photoemission spectroscopy. An energy gap opening in the topological surface-state bands of the three-dimensional topological insulator Bi₂Se₃ is observed due to the hybridization of the top and bottom surfaces. The drastic change in the shape of the band structure and the reversal of the size of the energy gap between 2 and 3 quintuple layer (QL) films indicate that the parity of the conduction and valence bands are exchanged by finite-size effects. The analyses based on an effective four-band model also support the occurrence of a quantum topological phase transition, thus, implying that 2 QL films are trivial while the 3 QL films are in the quantum spin Hall state.

DOI: 10.1103/PhysRevB.81.165432

PACS number(s): 73.20.-r, 75.70.Tj, 73.61.Ng

Topological insulators (TIs) are a novel state of quantum matter in three dimensions (3D) that have been gaining increased attention. Along with its two-dimensional (2D) counterpart, the quantum spin Hall (QSH) phase, they are mathematically characterized by the so-called Z_2 topological number.¹ While the bulk is insulating, there is a metallic edge or surface state which is topologically protected and hence robust against weak perturbation or disorder. Nowadays many experimental works have confirmed the existence of TI or QSH phase as well as the topologically protected nature of the edge states.²⁻⁷ Furthermore, materials that exhibit superconductivity by carrier doping into a TI (Cu_xBi₂Se₃) has been found⁸ and the relation between the topological surface states and Cooper pair formation is an intriguing challenge left to clarify.⁹

One of the important aspects in the study of TIs is the phase transition between the trivial (normal) and the topological state.^{10,11} The principal issue here is the exchange of the parity of conduction and valence bands by changing some external parameter. For example, by alloying Bi with Sb, it was shown that a trivial-to-non-trivial phase transition will occur theoretically¹² and has been indeed observed experimentally.¹³ In this case, the strength of the spin-orbit coupling is manipulated and results in the parity exchange. Another example is the case of HgTe/CdTe quantum well. In this case, it was reported that by reducing the thickness of the well below a critical thickness of $d_c=60$ Å, the inverted band gap of the bulk ($\Delta < 0$) once closes ($\Delta = 0$) and becomes a normal band gap ($\Delta > 0$),^{4,14} as schematically shown in Fig. 1(a). Thus, changing the system size can lead to a change in the parity. Similar size effects have been reported for Bi, where the trivial 3D bulk becomes a 2D QSH phase by making a single bilayer Bi film, which has yet to be realized experimentally.¹⁵ Therefore, reducing the system size and changing the dimensionality does not only have the advantage that the surface sensitivity is enhanced which will make the surface-state property more apparent in terms of 3D TI,¹⁶ but is also important in determining if the system is trivial or topological in 2D (Fig. 1).

Bulk Bi₂Se₃ is a 3D topological insulator with an inverted band gap whose band structure can be expressed by a four-band effective model.¹⁷ The surface states possess a linear

band dispersion expressed by the Dirac equation [Fig. 1(b)]. In a recent theoretical work, it was shown that this Hamiltonian possesses a similarity to the 2D QSH effective Hamiltonian proposed in Ref. 14 for the HgTe quantum wells.^{18,19} In fact, the two Hamiltonians can be regarded as nearly the same in the ultrathin film limit. The authors predicted that an energy gap will open in the surface-state dispersion due to the interaction between the top and bottom surfaces. Moreover, there will be an oscillatory change in the parity of ultrathin Bi₂Se₃ and Bi₂Te₃ films by changing the film thickness in units of quintuple layers [1 quintuple layer (QL) is the stack of two Bi and three Se or Te layers]. In another theoretical work (Ref. 20), it was shown that the inverted gap will close at $d_c=25$ Å for Bi₂Se₃, and below d_c a normal band gap will develop so the system will become trivial [Fig. 1(a)]. Therefore, a topological quantum phase transition is predicted to occur in the thin-film limit. However, this has not been experimentally demonstrated yet.

In the present work, we have performed angle-resolved photoemission spectroscopy (ARPES) measurements on ultrathin Bi₂Se₃ films to verify if the phase transition actually takes place. Although the sign of the energy gap cannot be determined from ARPES, we have found that the size of the energy gap is larger for the 3 QL (1 QL=9.5 Å) film com-

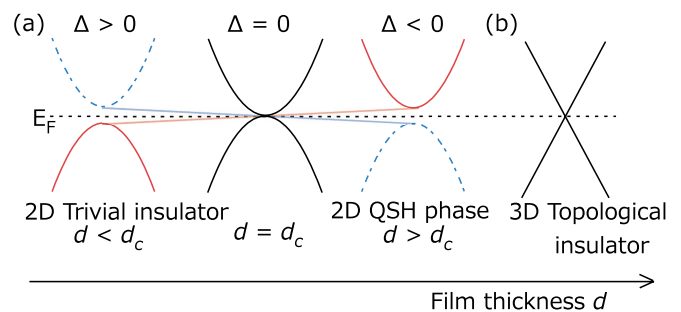


FIG. 1. (Color online) (a) Schematic of the topological quantum phase transition in 2D from the QSH state ($d > d_c$) to the trivial insulator ($d < d_c$) by reducing the film thickness. At $d = d_c$, the band gap closes and the parity of the conduction and valence bands is exchanged. (b) Schematic of the surface-state linear band dispersion of the 3D topological insulator.

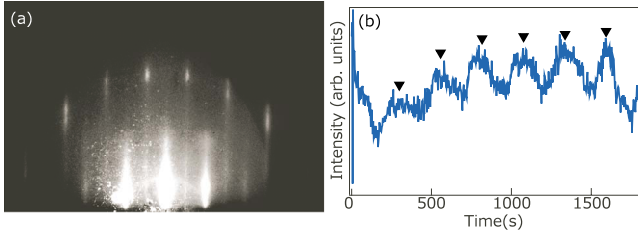


FIG. 2. (Color online) (a) A RHEED pattern of a 10 QL (95 Å) thick Bi_2Se_3 . The electrons are incident along the $[11\bar{2}]$ direction of the underlying Si substrate and the energy is 15 keV. (b) RHEED spot intensity of the (00) spot during Bi_2Se_3 growth showing clear oscillation and quintuple-layer by quintuple-layer growth.

pared to that of the 2 QL film. The shape of the band dispersion shifts dramatically by changing the film thickness from 2 QL to 3 QL. Furthermore, our quantitative analyses based on the theoretical work concerning the Hall conductance corroborates the above fact,²⁰ providing spectroscopic evidence that the quantum topological phase transition has actually occurred.

The ARPES experiments were performed at BL-5U of UVSOR using an electron analyzer of MBS-Toyama A-1. The energy and the angular resolutions were 20 meV and 0.2° , respectively. The photon energy used was $h\nu=20$ eV and the measurements were done at 10 K. The samples were fabricated in a method similar to the report of Ref. 21. First, a clean Si(111)- 7×7 surface was prepared on an *n*-type substrate (P-doped, 1–10 Ω cm at room temperature) by a cycle of resistive heat treatments. The Si(111) $\beta\sqrt{3}\times\sqrt{3}$ -Bi surface was formed by 1 ML (7.83×10^{14} cm⁻²) of Bi deposition on the 7×7 surface at 620 K monitored by reflection

high-energy electron diffraction (RHEED). Then Bi was deposited on the $\beta\sqrt{3}\times\sqrt{3}$ -Bi structure at ~ 400 K in a Se-rich condition. Such a procedure is reported to result in a smooth epitaxial film formation with the stoichiometric ratio of Bi:Se=2:3.²¹ Figure 2(a) shows the RHEED pattern of the Bi_2Se_3 film showing a clear 1×1 periodicity (the electron incidence is along the $[11\bar{2}]$ direction and the electron energy is 15 keV). The lattice constant was confirmed to be consistent with the bulk value of Bi_2Se_3 (4.14 Å) within the experimental error from comparison with the pattern of the Si(111)- 7×7 surface. It is also known that the minimum film thickness that can be achieved in this method is 1 QL, and the films can be formed QL-by-QL. We have indeed observed this QL-by-QL growth by monitoring the (00) spot intensity of the RHEED pattern of Fig. 2(a) with a charge-coupled device camera. As shown in Fig. 2(b), clear oscillations can be noticed and the film thicknesses can be determined from the number of peaks.

Figures 3(a)–3(d) show the dispersion images obtained by ARPES for the 1 (a), 2 (b), 3 (c), and 8 (d) QL thick Bi_2Se_3 films taken along the $\bar{\Gamma}$ - \bar{K} direction, respectively. For the 8 QL film (d), the band dispersion is similar to the one reported for a single crystal bulk² showing surface states that have Dirac-like linear dispersion as well as a bulk band just below E_F with strong intensity. It should be noted that even though Bi_2Se_3 is said to be an insulator, the bulk bands appear below the Fermi level E_F likely due to Se site defects.³ One difference that can be noticed between the single crystal bulk case and the 8 QL ultrathin film is the position of the Dirac point (E_D); for the bulk crystal case, it was reported that E_D is 0.3 eV below E_F , whereas $E_D=0.41$ eV in Fig. 3(d). This shift may be attributed to increased Se defects in the film or the

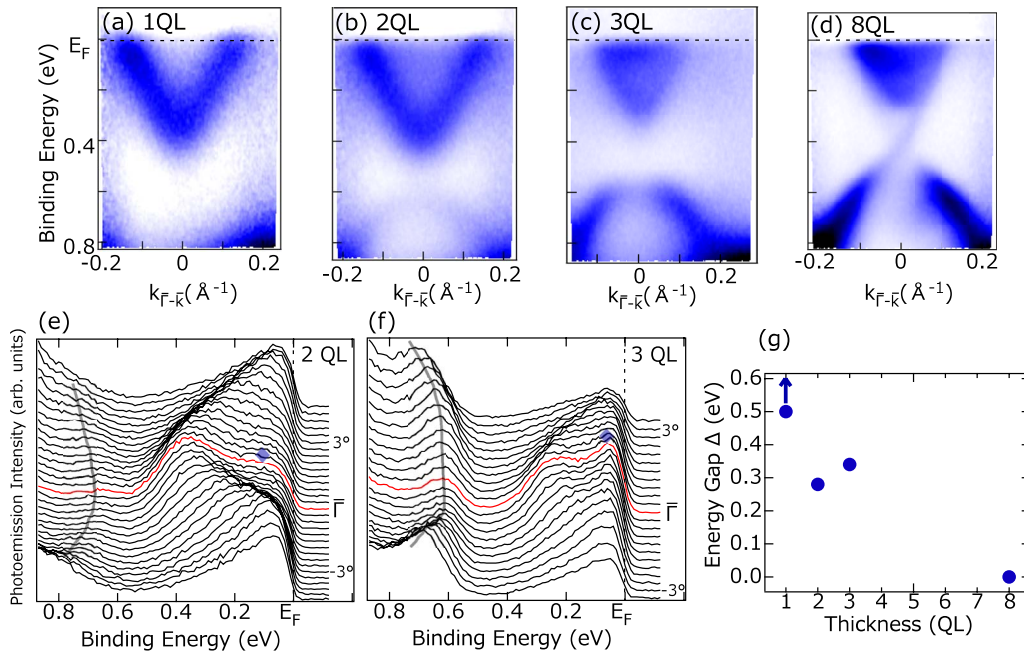


FIG. 3. (Color online) [(a)–(d)] E - k band dispersion images for the 1 QL (a), 2 QL (b), 3 QL (c), and 8 QL (d) ultrathin Bi_2Se_3 films along the $\bar{\Gamma}$ - \bar{K} direction near the $\bar{\Gamma}$ point, respectively. [(e) and (f)] Raw ARPES data for the 2 QL (e) and 3 QL (f) films near the $\bar{\Gamma}$ point. The diamonds show the bulk (quantum well) states. (g) The gap size deduced from the ARPES spectra of (a)–(f) plotted as a function of film thickness. The photon energy was $h\nu=20$ eV.

effect of enhanced band bending caused by the substrate.

Now let us look closely at the films that have different band dispersions. The spectra of 1 QL film [Fig. 3(a)] exhibit a single V-shaped metallic band. For the 2 QL film [Fig. 3(b)], the V-shaped band remains and another band below it appears. These two bands are likely the surface states that emerge as a result of the interaction of the two surfaces shown in Fig. 1, and we will refer to them as the “upper” and “lower” surface states. The lower surface state also has an inverted V shape. The energy gap Δ between the two bands at the $\bar{\Gamma}$ point is 0.28 eV as can be recognized from the raw spectra in Fig. 3(e). There is another state just below E_F that shows little dispersion [indicated by the diamond in Fig. 3(e)] and this is possibly a bulk or quantum-well state. At 3 QL [Fig. 3(c)], the shapes of the upper and lower surface states change drastically. The Fermi wave number of the upper states becomes about half as that in the 2 QL case and the shape of the lower band can be more described as an inverted U shape rather than a V shape. This can also be found in the raw spectra shown in Fig. 3(f); the peak positions for the lower surface states are nearly the same for the spectra just near the $\bar{\Gamma}$ point. The intensity of the bulk band just below E_F becomes much stronger than that of the 2 QL film resembling the 8 QL film. Furthermore, Δ is 0.34 eV in Figs. 3(c) and 3(f) for the 3 QL film, larger than that of the 2 QL film. The gap size dependence on the film thickness is summarized in Fig. 3(g). For the 1 QL film, we suspect that the gap is larger than 0.5 eV because only one band was observed within our measurement range. As for the 8 QL film, there was no gap observed. In the usual quantum-size effect picture, we expect that the gap size should decrease monotonically as the film thickness is increased since the energy spacing between the states will become smaller. In contrast to this naive picture, we find a reversal in the size of the energy gap between the 2 and 3 QL films. Although the sign of the energy gap is impossible to identify with ARPES, this suggests that there is a gap inversion as shown in Fig. 1 and together with the fact that the band dispersion changes drastically by going from 2 to 3 QL, an occurrence of the topological quantum phase transition is indicated.

In order to gain further insight into the topological properties of the ultrathin Bi_2Se_3 films, we have performed a quantitative analyses based on the theoretical approach reported in Ref. 20. According to this work, the in-plane dispersion of the surface states for the 3D topological insulator in the ultrathin limit is expressed as

$$E_{\pm} = E_0 - Dk^2 \pm \sqrt{(v_F \hbar k)^2 + (\Delta/2 - Bk^2)^2}, \quad (1)$$

in which \pm represents upper and lower surface states, E_0 is the midgap position, v_F is the Fermi velocity, Δ is the energy gap, and D and B are the coefficients that arise in the effective four-band model Hamiltonian shown in Ref. 17. The images of Figs. 3(b)–3(d) have been fitted using Eq. (1). The values of E_0 and $\Delta(>0)$ have been determined from the spectra at normal emission in Figs. 3(b)–3(f) and B , D , and v_F were adopted as the fitting parameters. For the 8 QL film, $B=0$ and $\Delta=0$ were also fixed to reproduce the linear dispersion near the $\bar{\Gamma}$ point. Figure 4 shows the fitted curves

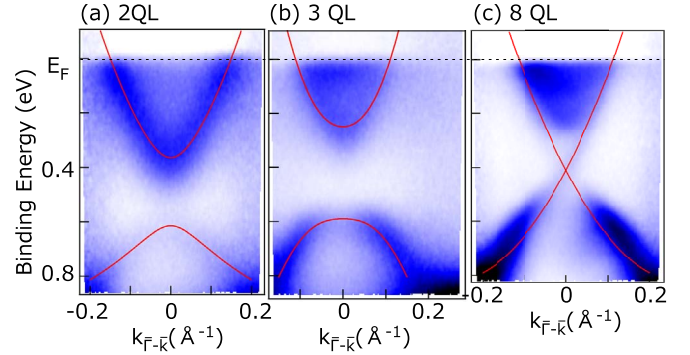


FIG. 4. (Color online) The band dispersion image overlapped with the fitted curves using Eq. (1).

overlapped on the band dispersion images and the fitting parameters are shown in Table I. The error bars show the difference of the fitted results for the upper and lower branches as well as the discrepancy of the fitted results using peak positions determined by energy and momentum distribution curves.²² The value of v_F in Table I is slightly smaller than the value reported for that of the bulk crystal² (5×10^5 m/s) and that of the theoretical work²¹ (6.2×10^5 m/s).

Now let us discuss the Hall conductance of the films which can be written as

$$\sigma_{xy} = -\frac{e^2}{2h} [\text{sgn}(\Delta) + \text{sgn}(B)]. \quad (2)$$

The above expression can be obtained utilizing the Kubo formula in the effective four-band model of Ref. 20 at zero temperature when the Fermi level lies between the energy gap. Thus, when Δ and B have the same signs, $|\sigma_{xy}| = e^2/h$. This means that there is finite Hall conductance even when the Fermi level is inside the band gap, implying the presence of gapless helical edge states. This situation can be regarded as a quantum spin Hall state. On the other hand, when the signs of Δ and B are different, $\sigma_{xy} = 0$ and there are no edge states. This corresponds to the case of a trivial insulator. Looking at Table I, we notice that for the 2 QL film, Δ and B have opposite signs whereas for the 3 QL film, the signs of Δ and B are the same. This implies that the 3 QL can be considered as an (n -doped) QSH, while the 2 QL film is an (n -doped) trivial insulator. The energy gap likely closes between the two thicknesses and a reversal of the parity of the

TABLE I. The fitted parameters using Eq. (1) for the 2, 3, and 8 QL ultrathin Bi_2Se_3 films.

	2 QL	3 QL	8 QL
E_0 (eV)	0.49	0.42	0.41
Δ (eV)	0.28	0.34	0
B (eV \AA^2)	-5.2 ± 3.0	18.0 ± 3.5	0
D (eV \AA^2)	-4.7 ± 2.0	-6.0 ± 2.0	-5.5 ± 2.0
v_F (10^5 m/s)	3.0 ± 0.3	4.4 ± 0.5	4.6 ± 0.5

conduction and valence bands seems to have indeed taken place as shown in Fig. 1(a).

Recently similar measurements were performed for Bi_2Se_3 films formed on epitaxial graphene on a SiC substrate.²³ By applying similar analyses to their results, we can say that even for the 2 QL films the topologically protected nature is conserved in contrast to our conclusion. While the details are unknown, we believe that this is due to the difference in the strength of the film-substrate interaction. In fact the authors have insisted that due to the large film-substrate interaction, the bands will show a large Rashba splitting which is not observed in the present case [Figs. 3(a)–3(d)]. Our films are mostly likely close to free-standing films for which the calculations have been performed.^{18–20} Unraveling the effect of the substrate in the topological nature of these films remains to be a very important future work.

It should be emphasized that although our ARPES spectra show the signature of the topological quantum phase transition, it is still only indirect evidence. The presence of metallic edge states as well as their role in the transport properties of the system must be verified before a definite conclusion can be made. After a method is established to make the bulk states of these films really insulating, transport measure-

ments similar to those reported in Refs. 4 and 5 will provide direct evidence of the edge states. Future scanning tunneling microscopy/scanning tunneling spectroscopy (STM/STS) studies near the edge of the terrace of an ultrathin film will also provide direct proof.

In conclusion, we have performed ARPES measurements on ultrathin Bi_2Se_3 films formed on the $\text{Si}(111)\beta\sqrt{3}\times\sqrt{3}$ -Bi surface. We observed a gap opening in the topological surface state bands of bulk single crystal Bi_2Se_3 due to the interaction of the top and bottom surfaces. The drastic change in the band dispersion, reversal of the size of the energy gap, and the analyses considering the finite-size effects in the four-band effective model all indicated the occurrence of a quantum topological phase transition between 2 and 3 QL films; the 2 QL films are trivial while the 3 QL films can be regarded as a quantum spin Hall state. It will be interesting to confirm our spectroscopic implications with future STM/STS and transport studies.

This work was supported by Grants-In-Aid from the Japanese Society for the Promotion of Science. The ARPES experiments were performed under the proposal numbers of UVSOR 21-524 and 22-521.

*hirahara@surface.phys.s.u-tokyo.ac.jp

¹C. L. Kane and E. J. Mele, *Phys. Rev. Lett.* **95**, 146802 (2005).

²Y. Xia, D. Qian, D. Hsieh, L. Wray, A. Pal, H. Lin, A. Bansil, D. Grauer, Y. S. Hor, R. J. Cava, and M. Z. Hasan, *Nat. Phys.* **5**, 398 (2009).

³D. Hsieh, Y. Xia, D. Qian, L. Wray, J. H. Dil, F. Meier, J. Osterwalder, L. Patthey, J. G. Checkelsky, N. P. Ong, A. V. Fedrov, H. Lin, A. Bansil, D. Grauer, Y. S. Hor, R. J. Cava, and M. Z. Hasan, *Nature (London)* **460**, 1101 (2009).

⁴M. König, S. Wiedmann, C. Brüne, A. Roth, H. Buhmann, L. W. Molenkamp, X.-L. Qi, and S.-C. Zhang, *Science* **318**, 766 (2007).

⁵A. Roth, C. Brüne, H. Buhmann, L. W. Molenkamp, J. Maciejko, X.-L. Qi, and S.-C. Zhang, *Science* **325**, 294 (2009).

⁶P. Roushan, J. Seo, C. V. Parker, Y. S. Hor, D. Hsieh, D. Qian, A. Richardella, M. Z. Hasan, R. J. Cava, and A. Yazdani, *Nature (London)* **460**, 1106 (2009).

⁷T. Zhang, P. Cheng, X. Chen, J.-F. Jia, X. Ma, K. He, L. Wang, H. Zhang, X. Dai, Z. Fang, X. Xie, and Q.-K. Xue, *Phys. Rev. Lett.* **103**, 266803 (2009).

⁸Y. S. Hor, A. J. Williams, J. G. Checkelsky, P. Roushan, J. Seo, Q. Xu, H. W. Zandbergen, A. Yazdani, N. P. Ong, and R. J. Cava, *Phys. Rev. Lett.* **104**, 057001 (2010).

⁹L. Wray, S. Xu, J. Xiong, Y. Xia, D. Qian, H. Lin, A. Bansil, Y. Hor, R. Cava, and M. Hasan, [arXiv:0912.3341](https://arxiv.org/abs/0912.3341) (unpublished).

¹⁰S. Murakami, S. Iso, Y. Avishai, M. Onoda, and N. Nagaosa, *Phys. Rev. B* **76**, 205304 (2007).

¹¹S. Murakami, *New J. Phys.* **9**, 356 (2007).

¹²L. Fu and C. L. Kane, *Phys. Rev. B* **76**, 045302 (2007).

¹³D. Hsieh, D. Qian, L. Wray, Y. Xia, Y. S. Hor, R. J. Cava, and M. Z. Hasan, *Nature (London)* **452**, 970 (2008).

¹⁴B. A. Bernevig, T. L. Hughes, and S.-C. Zhang, *Science* **314**, 1757 (2006).

¹⁵D. B. Dougherty, P. Maksymovych, J. Lee, and J. T. Yates, *Phys. Rev. Lett.* **97**, 236806 (2006).

¹⁶T. Hirahara, Y. Sakamoto, Y. Saisyu, H. Miyazaki, S. Kimura, T. Okuda, I. Matsuda, S. Murakami, and S. Hasegawa, *Phys. Rev. B* **81**, 165422 (2010).

¹⁷H. Zhang, C.-X. Liu, X.-L. Qi, X. Dai, Z. Fang, and S.-C. Zhang, *Nat. Phys.* **5**, 438 (2009).

¹⁸C.-X. Liu, H. J. Zhang, B. Yan, X.-L. Qi, T. Frauenheim, X. Dai, Z. Fang, and S.-C. Zhang, *Phys. Rev. B* **81**, 041307(R) (2010).

¹⁹J. Linder, T. Yokoyama, and A. Sudbø, *Phys. Rev. B* **80**, 205401 (2009).

²⁰H.-Z. Lu, W.-Y. Shan, W. Yao, Q. Niu, and S.-Q. Shen, *Phys. Rev. B* **81**, 115407 (2010).

²¹G. Zhang, H. Qin, J. Teng, J. Guo, X. Dai, Z. Fang, and K. Wu, *Appl. Phys. Lett.* **95**, 053114 (2009).

²²T. Hirahara, I. Matsuda, M. Ueno, and S. Hasegawa, *Surf. Sci.* **563**, 191 (2004).

²³Y. Zhang, K. He, C. Z. Chang, C. L. Song, L. L. Wang, X. Chen, J. F. Jia, Z. Fang, X. Dai, W. Y. Shan, S. Q. Shen, Q. Niu, X. L. Qi, S. C. Zhang, X. C. Ma, and Q. K. Xue, [arXiv:0911.3706](https://arxiv.org/abs/0911.3706) (unpublished).